ChemComm

COMMUNICATION

View Article Online
View Journal | View Issue

Cite this: *Chem. Commun.*, 2023, 59, 11955

Received 22nd August 2023,
Accepted 10th September 2023

DOI: 10.1039/d3cc04062c

rsc.li/chemcomm

Continuous magnetic separation microfluidic chip for tumor cell *in vivo* detection†

Man Tang, ‡[ab] Jiao Feng,‡[a] Hou-Fu Xia,[c] Chun-Miao Xu,[a] Ling-Ling Wu,[a] Min Wu,[c] Shao-Li Hong,[a] Gang Chen*[c] and Zhi-Ling Zhang *[a]

Continuously recording the dynamic changes of circulating tumor cells (CTCs) is crucial for tumor metastasis. This paper creates a continuous magnetic separation microfluidic chip that enables rapid and continuous *in vivo* cell detection. The chip shows its potential to study tumor cell circulation in the blood, offering a new platform for studying the cellular mechanism of tumor metastasis.

Circulating tumor cells (CTCs) are an important medium for cancer metastases, but they are extremely rare in the blood.[1,2] As demonstrated in many clinical cases, no more than 10 CTCs can be found in 7.5 mL of blood from cancer patients, especially for early-stage cancer patients.[3,4] Therefore, the majority of studies on CTC detection are focused on increasing sensitivity or specificity.[5–7] Due to the concern for patient safety, CTC detection is still limited to small blood volume (usually 1–10 mL).[8–10] A small blood sample means few CTCs may be found, which leads to false negative results, causing further studies to be difficult to process with the existing method.

Nowadays, an *in vivo* detection strategy that processes large blood volumes directly from the blood vessel exhibits great potential.[11] This technology samples a large volume of blood (several milliliters or even liters), and hence almost all the CTCs in the vessel can be found. One of the popular strategies is to insert an intravenous stainless steel medical wire into the vein.[12–14] After coating with antibodies against epithelial cellular adhesion molecule (EpCAM) protein, CTCs can be captured *in vivo*.[15] However, the captured tumor cells might be lost when the wire is extracted from the vein, which further influences the detection efficiency. Another *in vivo* flow cytometry-based technology (IVFC) is a powerful method for detecting and monitoring CTCs quantitatively.[16,17] The evolved technology is mainly used for real-time studying the influence of tumor progression. But an apparent limitation is that the CTCs cannot be acquired for further investigation. Inspired by the extracorporeal circulation, some microfluidic chip-based *in vivo* detection technology was developed.[18,19] Taking advantage of the microfluidic chip, the whole blood is extracted from the vessel by a pump, then flows through the microfluidic chip-based sensing system for CTC capture and detection.[20] After that, the blood continues to flow back into the patient and the circuit will repeat. However, these methods usually involve the pre-injection of antibody-coated nanomaterial into the vessel, and the biosafety of nanomaterials remains to be verified.

Previously, we have constructed a magnetic chip-based extracorporeal circulation for *in vivo* CTC detection.[21–23] Taking a C57BL/6 mouse as a model, the immunomagnetic separation-based system was stable, safe, and exhibited a higher capture efficiency than the *ex vivo* method. However, to increase the temporal resolution in monitoring the natural CTC cleanup process *in vivo*, the throughput of this method needed to be improved. Some research showed that continuous-flow separation normally had a high throughput with high precision, which was suitable for real-time monitoring or continuously separating target biomarkers.[24,25] In this work, we designed a magnetic separation microfluidic chip that can continuously collect the tumor cells directly from the blood. By regulating the magnetic field distribution in a microfluidic chip, magnetic nanoparticles (MNs) can realize functions like magnetic lateral, tumor cell tagged, and recovery respectively. Using the laminar flow effect of the microfluidic chip, antibody-modified MN injection was processed as a function of magnetophoresis driven by a permanent magnet. Then there was a reaction area for sufficient contact between the MNs and tumor cells in the whole blood. After that, the magnetically tagged tumor cells and the excess of unreacted MNs were completely recovered

[a] *College of Chemistry and Molecular Sciences, Wuhan University, Wuhan 430072, P. R. China. E-mail: zlzhang@whu.edu.cn*
[b] *School of Electronic and Electrical Engineering, Wuhan Textile University, Wuhan 430200, P. R. China*
[c] *The State Key Laboratory Breeding Base of Basic Science of Stomatology (Hubei-MOST) and Key Laboratory of Oral Biomedicine of Ministry of Education, School and Hospital of Stomatology, Wuhan University, Wuhan 430079, P. R. China. E-mail: geraldchan@whu.edu.cn*

† Electronic supplementary information (ESI) available. See DOI: https://doi.org/10.1039/d3cc04062c

‡ These authors contributed equally to this work.

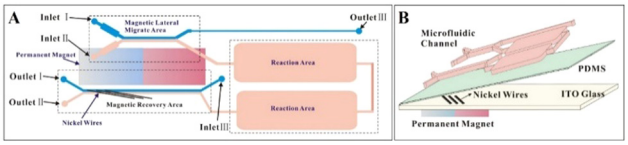

Scheme 1 Schematic diagram of the design for the continuous magnetic microfluidic chip. (A) The working principle of the continuous magnetic microfluidic chip. Inlet I is used for MN introduction. Inlet II is used for sample introduction, and Inlet III is used for PBS introduction. On the other side, outlet I is used for tumor cell and MN recovery. Outlet II is for the sample, and outlet III is for waste. (B) Schematic diagram of the integrated continuous magnetic microfluidic chip. There are three layers in the chip: the bottom layer is ITO glass with two magnets fixed under it, the middle layer is electroplated with several nickel wires and encapsulated in a thin PDMS film, and the upper layer is a microfluidic channel made by electroplating.

with the help of a series of nickel wires under the microchannel. This chip achieved about 95.05% cell capture efficiency *ex vivo* with high universality and specificity. Moreover, up to 98% of the MNs could be recovered, which prevented the probable harm to lives in subsequent *in vivo* experiments. Then, the natural CTC cleanup process was mimicked and continuously monitored, and a process in which the cell numbers increased rapidly and then decreased gradually was discovered, which was consistent with those reported previously.

The design of the continuous magnetic separation microfluidic chip contains three areas, as illustrated in Scheme 1A. Immunomagnetic nanoparticles (IMNs, coated with anti-EpCAM antibody, Fig. S1, ESI†) and samples (such as tumor cells or the blood sample) are introduced into the chip separately from inlets I and inlets II, respectively. In the beginning, both the IMNs and samples will remain pristine due to the laminar flow effect in the microfluidic chip. Meanwhile, under the guidance of the magnetic field, IMNs will transport to the sample and flow together into the reaction area. Furthermore, IMNs can contact and react with the tumor cells in the sample, and thus the tumor cells are magnetically tagged. In this work, two reaction areas of the same size (20 mm in length and 7 mm in width) are designed to ensure sufficient contact between the tumor cells and the IMNs. After that, the tagged tumor cells are recovered in the magnetic recovery area for further study. To simplify the chip, both the recovery area and the magnetic lateral area share the same external magnetic field. But different from the function of the magnetic lateral area, the recovery area needs to ensure that the magnetically tagged tumor cells and IMNs are completely recovered; hence, the magnetic force of the magnetically tagged tumor cells and IMNs needs to be increased appropriately. Nickel has a higher permeability compared to the buffer, so it can produce a strong magnetic field under the function of an external magnet.[26] Encouraged by this property, nickel wires are set under the magnetic recovery area to improve the recovery efficiency. In this way, almost all the magnetically tagged tumor cells and unreacted IMNs will be recovered (Fig. S2C, ESI†). The rest of the blood sample is unaffected and eventually collected for further study. Experiment results shown in Fig. S2 (ESI†) confirmed that this chip can accurately regulate and control the motion of IMNs, which serves as an important basis for *in vivo* tumor cell detection and monitoring.

To obtain better cell detection results, the detailed structure of the microfluidic chip (like the heights of the reaction area and the angle of inclination of the nickel wires) and the experimental parameters (like the flow rate conditions in each inlet) were carefully optimized (Fig. S3, ESI†). After that, the specificity of this continuous magnetic separation chip was further investigated. Fig. 1A showed that this chip could barely capture the EpCAM-negative cells, such as Jurkat T cells. Also, MNs without antibody modification were unable to capture the MCF-7 cells. Moreover, the data revealed that cell detection depended on the presence of an external magnetic field in this chip. These results confirmed the specific binding between IMNs and tumor cells.

On the other hand, the capture efficiencies of the continuous magnetic separation chip towards different kinds of epithelial original tumor cells (SK-BR-3 breast cells, Hep G2 hepatoma carcinoma cells, and MDA-MB-453 breast cells) were investigated. Epithelial tumor cells with EpCAM expression could be well captured by the chip with efficiencies up to 90% (Fig. 1B). The above finding demonstrated that this continuous magnetic separation chip could be applied to capture tumor cells from different types of hematogenous metastatic tumors.

For further use in *in vivo* detection, the tumor cell capture ability of this continuous magnetic separation chip in the whole blood needed to be investigated. As the component of blood was complex, the dispersion of the IMNs is a guarantee of subsequent cell detection and should be investigated first. As shown in Fig. 2A–C, the hydrodynamic size of the MNs after a magnetic lateral migration remained almost constant either in PBS or in whole blood. The polymer dispersity indexes (PDIs) of the MNs were both less than 0.1 whether in PBS or blood, demonstrating that the MNs kept evenly dispersed after magnetic lateral migration, which laid the foundation for the following CTC *in vivo* detection.

Besides that, the capture efficiencies of the microfluidic chip towards MCF-7 cells in the blood were verified. Experiment results demonstrated that the MCF-7 cell capture efficiency kept up to 87% and about 98.5% IMNs could be recovered

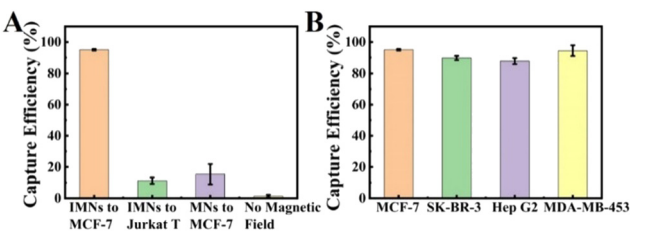

Fig. 1 (A) Capture efficiencies of IMNs towards MCF 7 cells, IMNs towards Jurkat T cells, MNs towards MCF 7 cells, and IMNs towards MCF 7 cells without a magnetic field. (B) The capture efficiencies of the IMN towards MCF 7 cells, SK-BR-3 cells, Hep G2 cells, and MDA-MB-453 cells, respectively. The error bars indicate the standard deviation of three experiments.

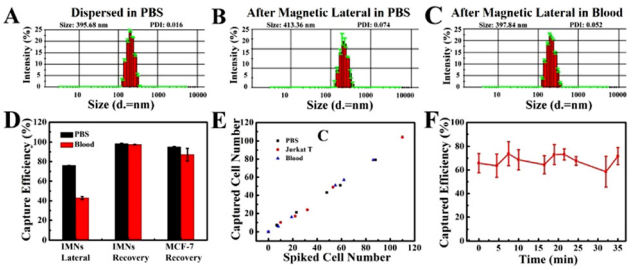

Fig. 2 (A) The hydrodynamic size of the MNs in PBS. (B) The hydrodynamic size of the MNs after magnetic lateral migration in the microfluidic chip. (C) The hydrodynamic size of the MNs after magnetic lateral migration in microfluidic filled by the whole blood. (D) Capture efficiency in PBS and the whole blood of the IMNs in the lateral area, the IMNs in the recovery area, and MCF-7 cells in the recovery area, respectively. (E) Capture efficiencies of the continuous magnetic separation chip towards MCF-7 cells at different cell numbers in three different types of samples: PBS (■), a mixture with Jurkat T cells (●), and whole blood (▲), respectively. (F) Capture efficiencies of the magnetic microfluidic chip at different time points within 35 minutes, the collection time at each time point was set as 1 minute. The error bars indicate the standard deviation of three experiments.

from the chip (Fig. 2D). Compared to the results in PBS, the recovery efficiency of IMNs in blood was nearly the same but the cell capture efficiency in blood was slightly reduced. This result might be explained as the presence of a huge number of cells in the whole blood affected the IMN transport efficiency. Since there is an obvious IMN lateral efficiency reduced in the magnetic lateral area. Even though, the number of IMNs was vastly excessive, hence the decrease in the cell capture efficiency was not significant. These results showed the excellent anti-interference ability in the blood of this continuous magnetic separation chip.

CTCs are rare events in the blood. Hence about 0-100 MCF-7 cells were spiked into PBS, Jurkat T cells, and whole blood, respectively, to simulate this situation. The results showed that the disturbance from Jurkat T cells or blood cells had little influence on the capture efficiency towards MCF-7 cells (Fig. 2E). Regression analyses of the number of captured cells *versus* the total number of spiked cells were obtained: $y = 0.85x$ ($R^2 = 0.995$, in PBS), $y = 0.93x$ ($R^2 = 0.993$, in Jurkat T cells), $y = 0.92x$ ($R^2 = 0.999$, in the whole blood), showing that the continuous magnetic separation chip could efficiently capture tumor cells in the blood. Therefore, it could be further concluded that the complex conditions had little effect on the performance of this continuous magnetic separation chip.

To monitor the *in vivo* experiment, the ability of this magnetic separation chip to capture tumor cells continuously and repeatedly was studied. Unlike the *in vitro* experiment, a peristaltic pump was applied to drive fluid flow instead of the injection pump. Due to the instability of the peristaltic pump, two buffer areas were set next to both the inlet I and inlet II to reduce the influence of fluidic disturbance. Within 35 minutes, 10 time points were randomly selected and the MCF-7 cell capture efficiencies were all above 65% (Fig. 2F). This decrease might be due to the inconsistent flow from the peristaltic pump. Although decreased, the cell capture efficiency remained stable and effective for a longer time, so it could continue to be used for the following *in vivo* detection.

As a continued cell separation method, the recovered tumor cells from the continuous magnetic separation chip should be further collected and reserved for the following studies, like enumeration and cell identification. In this work, a single-cell array microfluidic chip was used to study the collected tumor cells at the single-cell level (Fig. S4, ESI†). The experiment results confirmed that the collected tumor cells kept cell activity, which was beneficial for the subsequent cell-related study (Fig. S5, ESI†). Moreover, this single-cell array chip can not only remove excess magnetic nanoparticles and blood cells but also be used for three-color immunocytochemical identification. In this way, the purity of the captured CTCs is significantly enhanced, and the identification results are simple and easy to distinguish.

In our previous work, the majority of the CTCs were cleared away in the first 10 minutes after they entered the blood circulation system.[25] Despite this observation, the detailed cell clearance process during the first 10 minutes remains unknown. However, it was very important to study the CTC secretion mechanism. Aimed at this, an *in vivo* microfluidic chip-based tumor cell detection system was constructed (Fig. 3A). This system consisted of a peristaltic pump, a continuous magnetic separation chip, and an about 5-to-8 weeks old C57BL/6 mouse (BALB/c background). The mouse was hocussed during the whole process of CTC *in vivo* detection.

The constructed microfluidic chip-based *in vivo* detection system was applied to monitor the simulative natural CTC clear-up process, especially in the first 20 minutes. This study was carried out according to the guidelines approved by the review board of the ethics committee of the Hospital of Stomatology, Wuhan University. Meanwhile, the study was performed according to the World Medical Association Declaration of Helsinki and the National Institutes of Health guidelines regarding the use of clinical tissues. Written informed consent was obtained from all the subjects in our research. For better observation, MCF-7 cells were stained with DAPI for the nucleus and DiI for cytomembrane before being injected into the mouse. Immediately, the cell number change was monitored every minute. As revealed by Fig. 3B, the number of captured MCF-7 cells sharply increased in the first 2 minutes. After that, the MCF-7 cell number gradually reduced and eventually

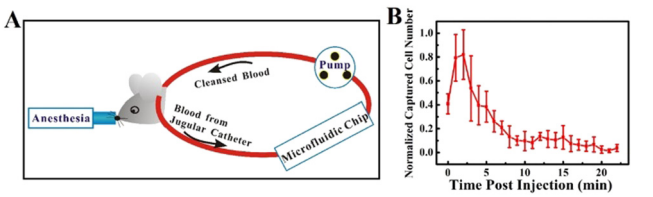

Fig. 3 (A) Diagram of the *in vivo* microfluidic chip-based CTC detection system. (B) Quantitative changes at different times after MCF 7 cells enter the bloodstream. The error bars indicate the standard deviation of three experiments.

stabilized to 10% of the maximum. This phenomenon was consistent with literature reports that circulating CT26 cells rapidly increased right after injection and quickly decreased to below 10% of the maximum within 2 minutes.[27,28] Compared to our previous work, this continuous magnetic separation microfluidic chip had a higher temporal resolution, exhibiting potential applications in CTC *in vivo* monitoring.

Microfluidic chips with precise magnetic field control enable MNs to perform various functions without manual intervention. In this work, we designed a magnetic microfluidic chip for the continuous collection and detection of tumor cells *in vivo*, which can be further used for *in vivo* tumor cell detection. This chip had a capture efficiency of 95.05% and could recover almost all the introduced IMNs from entering the living animal. For *in vivo* detection, the capture efficiency of the continuous magnetic separation microfluidic chip remained consistent over a long time, and hence it could serve as a good technology for tumor cell number monitoring. This chip was capable of studying the natural CTC cleanup process, indicating that it's an ideal platform for continuous separation and monitoring of tumor cell quantitative changes *in vivo*, which provided new technical support for CTC-related tumor monitoring and research.

The authors are thankful for the support of the National Natural Science Foundation of China (22274118, 22074107, and 22004094).

Conflicts of interest

The authors declare no competing financial interest.

Notes and references

1 M. Cristofanilli, *Semin. Oncol.*, 2006, **33**, S9–S14.
2 C. Alix-Panabières and K. Pantel, *Clin. Chem.*, 2013, **59**, 110–118.
3 S. Mocellin, D. Hoon, A. Ambrosi, D. Nitti and C. R. Rossi, *Clin. Cancer Res.*, 2006, **12**, 4605–4613.
4 J. B. Smerage and D. F. Hayes, *Br. J. Cancer*, 2006, **94**, 8–12.
5 Z. Shen, A. Wu and X. Chen, *Chem. Soc. Rev.*, 2017, **46**, 2038–2056.
6 L. Wu, H. Ding, X. Qu, X. Shi, J. Yang, M. Huang, J. Zhang, H. Zhang, J. Song, L. Zhu, Y. Song, Y. Ma and C. Yang, *J. Am. Chem. Soc.*, 2020, **142**, 4800–4806.
7 J. Lyu, H. Xu, B. Dong, C. Li, S. Yu, S. Hu, B. Zhou, L. Wang and H. Song, *Chem. Eng. J.*, 2022, **448**, 137761.
8 L. Zhu, H. Lin, S. Wan, X. Chen, L. Wu, Z. Zhu, Y. Song, B. Hu and C. Yang, *Anal. Chem.*, 2020, **92**, 15229–15235.
9 S. Nagrath, L. V. Sequist, S. Maheswaran, D. W. Bell, D. Irimia, L. Ulkus, M. R. Smith, E. L. Kwak, S. Digumarthy, A. Muzikansky, P. Ryan, U. J. Balis, R. G. Tompkins, D. A. Haber and M. Toner, *Nature*, 2007, **450**, 1235–1239.
10 S. L. Stott, C. H. Hsu, D. I. Tsukrov, M. Yu, D. T. Miyamoto, B. A. Waltman, S. M. Rothenberg, A. M. Shah, M. E. Smas, G. K. Korir, F. P. Floyd, Jr., A. J. Gilman, J. B. Lord, D. Winokur, S. Springer, D. Irimia, S. Nagrath, L. V. Sequist, R. J. Lee, K. J. Isselbacher, S. Maheswaran, D. A. Haber and M. Toner, *Proc. Natl. Acad. Sci. U. S. A.*, 2010, **107**, 18392–18397.
11 H. Pei, L. Li, Z. Han, Y. Wang and B. Tang, *Lab Chip*, 2020, **20**, 3854–3875.
12 O. Vermesh, A. Aalipour, T. J. Ge, Y. Saenz, Y. Guo, I. S. Alam, S.-M. Park, C. N. Adelson, Y. Mitsutake, J. Vilches-Moure, E. Godoy, M. H. Bachmann, C. C. Ooi, J. K. Lyons, K. Mueller, H. Arami, A. Green, E. I. Solomon, S. X. Wang and S. S. Gambhir, *Nat. Biomed. Eng.*, 2018, **2**, 696–705.
13 T. H. Kim, Y. Wang, C. R. Oliver, D. H. Thamm, L. Cooling, C. Paoletti, K. J. Smith, S. Nagrath and D. F. Hayes, *Nat. Commun.*, 2019, **10**, 1478.
14 S.-B. Cheng, M. Wang, C. Zhang, M.-M. Chen, Y.-K. Wang, S. Tian, N. Zhan, W.-G. Dong, M. Xie and W.-H. Huang, *Anal. Chem.*, 2020, **92**, 5447–5455.
15 D. Wang, C. Ge, W. Liang, Q. Yang, Q. Liu, W. Ma, L. Shi, H. Wu, Y. Zhang, Z. Wu, C. Wei, L. Huang, Z. Fang, L. Liu, S. Bao and H. Zhang, *Adv. Sci.*, 2020, **7**, 2000940.
16 I. Georgakoudi, N. Solban, J. Novak, W. L. Rice, X. Wei, T. Hasan and C. P. Lin, *Cancer Res.*, 2004, **64**, 5044–5047.
17 K. Pang, B. Gu, F. Liu, M. Dong, L. Zhu and X. Wei, *J. Innovative Opt. Health Sci.*, 2019, **12**, 1930008.
18 J. H. Kang, M. Super, C. W. Yung, R. M. Cooper, K. Domansky, A. R. Graveline, T. Mammoto, J. B. Berthet, H. Tobin, M. J. Cartwright, A. L. Watters, M. Rottman, A. Waterhouse, A. Mammoto, N. Gamini, M. J. Rodas, A. Kole, A. Jiang, T. M. Valentin, A. Diaz, K. Takahashi and D. E. Ingber, *Nat. Med.*, 2014, **20**, 1211–1216.
19 B. Hamza, S. R. Ng, S. M. Prakadan, F. F. Delgado, C. R. Chin, E. M. King, L. F. Yang, S. M. Davidson, K. L. DeGouveia, N. Cermak, A. W. Navia, P. S. Winter, R. S. Drake, T. Tammela, C. M. C. Li, T. Papagiannakopoulos, A. J. Gupta, J. S. Bagnall, S. M. Knudsen, M. G. Vander Heiden, S. C. Wasserman, T. Jacks, A. K. Shalek and S. R. Manalis, *Proc. Natl. Acad. Sci. U. S. A.*, 2019, **116**, 2232–2236.
20 N. Crawley, M. Thompson and A. Romaschin, *Anal. Chem.*, 2014, **86**, 130–160.
21 M. Tang, C.-Y. Wen, L.-L. Wu, S.-L. Hong, J. Hu, C.-M. Xu, D.-W. Pang and Z.-L. Zhang, *Lab Chip*, 2016, **16**, 1214–1223.
22 M. Tang, H.-F. Xia, C.-M. Xu, J. Feng, J.-G. Ren, F. Miao, M. Wu, L.-L. Wu, D.-W. Pang, G. Chen and Z.-L. Zhang, *Anal. Chem.*, 2019, **91**, 15260–15266.
23 J. Feng, C. M. Xu, H. F. Xia, H. M. Liu, M. Tang, Y. S. Tian, G. Chen and Z. L. Zhang, *Anal. Chem.*, 2023, **95**, 8735–8743.
24 R. Nasiri, A. Shamloo, S. Ahadian, L. Amirifar, J. Akbari, M. J. Goudie, K. Lee, N. Ashammakhi, M. R. Dokmeci, D. Di Carlo and A. Khademhosseini, *Small*, 2020, **16**, e2000171.
25 A. Mishra, T. D. Dubash, J. F. Edd, M. K. Jewett, S. G. Garre, N. M. Karabacak, D. C. Rabe, B. R. Mutlu, J. R. Walsh, R. Kapur, S. L. Stott, S. Maheswaran, D. A. Haber and M. Toner, *Proc. Natl. Acad. Sci. U. S. A.*, 2020, **117**, 16839–16847.
26 J. D. Adams, U. Kim and H. T. Soh, *Proc. Natl. Acad. Sci. U. S. A.*, 2008, **105**, 18165–18170.
27 H. Seo, Y. Hwang, K. Choe and P. Kim, *Biomed. Opt. Express*, 2015, **6**, 2158–2167.
28 C. M. Pitsillides, J. M. Runnels, J. A. Spencer, L. Zhi, M. X. Wu and C. P. Lin, *Cytometry, Part A*, 2011, **79**, 758–765.

